COMMUNICATIONS IN SCIENCE AND TECHNOLOGY
Homepage: cst.kipmi.or.id

Domestic waste (eggshells and banana peels particles) as sustainable and renewable resources for improving resin-based brakepad performance: Bibliometric literature review, techno-economic analysis, dual-sized reinforcing experiments, to comparison with commercial product

Asep Bayu Dani Nandiyanto[a,*], Risti Ragadhita[a], Meli Fiandini[a], Dwi Fitria Al Husaeni[a], Dwi Novia Al Husaeni[a], Farid Fadhillah[b]

[a]*Universitas Pendidikan Indonesia, Jl. Setiabudi No. 229, Bandung, Indonesia*
[b]*Chemical Engineering Department, Al Imam Mohammad Ibn Saud Islamic University, Riyadh, Saudi Arabia, 11432, Saudi Arabia*

Article history:
Received: 14 March 2022 / Received in revised form: 14 June 2022 / Accepted: 16 June 2022

Abstract

The objective of this study is to develop a new environmentally-friendly brake pad made from eggshells (Es) and banana peels (BPs) as reinforcement agents. E and BP particles as dual reinforcement with various compositions were combined. The E/BP mixture was then embedded on a polymer matrix composing a resin/hardener mixture in a 1:1 ratio. As a standard, brake pads using a single reinforcement of E and BP particles were also fabricated. Physical properties (i.e. particle size, surface roughness, morphology, and density), as well as mechanical properties (i.e. hardness, wear rate, and friction coefficient properties) were investigated. It was observed that using dual reinforcements was preferable (compared to using single reinforcements) because they had a synergistic effect on the mechanical properties of the brake pad. The best mechanical properties were found in dual reinforcements of brake pad specimens using E/BP particles with a higher BP ratio in which the value of the stiffness test, puncture test, wear rate, and coefficient of friction were 4.5 MPa, 86.80, 0.093×10^{-4} g/s.mm^2, and 1.67×10^{-4}, respectively. A high BP particle ratio played a dominant role in dual reinforcements, increasing the resin's bonding ability and resulting in good adhesion between the reinforcement and matrix. When compared to commercial brake pads, the brake pad specimens fabricated in this study met the standards. The techno-economic analysis also confirmed the prospective production of brake pads from E and BP particles (compared to commercial brake pads). From this research, it is expected that environmentally friendly and low-cost brake pads can be used to replace the dangerous friction materials.

Keywords: Agricultural waste; brake pad; banana peel; eggshell; and natural fiber

1. Introduction

A brake pad is a braking system that is used on all vehicles. Brake pads are classified into three types: metallic, organic, and ceramic. Brake pads are one of the prospective components in industries. The automotive brake pads market surpassed USD 3 billion in 2021 and is expected to grow at a compound annual growth rate (CAGR) of 4.3% between 2022 and 2028. The industry's shipments are expected to exceed 728,625.8 thousand units by 2028. Increases in vehicle sales, as well as the availability of advanced and lightweight friction materials, are expected to drive demand for automotive brake pads [1].

Commercially available brake pads are typically made of asbestos fiber embedded in a polymer matrix with other four constituent materials such as binders, fillers, friction materials, and reinforcement [2]. Asbestos is used because of its heat resistance. However, the use of asbestos in any forms was prohibited beginning in the 1970s due to its carcinogenic nature. As a result of the asbestos ban, there have been numerous widespread complaints about the difficulty in finding a substitute for asbestos [3]. Considering the risk to one's health, non-carcinogenic brake pads must be made from alternative materials [4]. For this. high-performance, asbestos-free brake linings are being developed.

Several previous studies have resulted in the development of brake pads made of agricultural waste. Agricultural waste is used as an alternative to asbestos material in brake pads due to its abundant availability, affordability and possibility to be one of the steps to manage the problems of agricultural waste (Environmental Preservation) [2,5-8]. Although the new brake pad developed from agricultural waste does not contain asbestos, it must meet requirements in the automotive sector such as stable friction coefficient and lower wear rate at various operating speeds, pressures, temperatures, and environmental conditions [9]. Therefore, it is important to select materials or a combination of materials from agricultural waste to meet the requirements of the brake pad. Nandiyanto et al. [10] developed

* Corresponding author.
Email: nandiyanto@upi.edu
https://doi.org/10.21924/cst.7.1.2022.757

a rice husk-based brake pad with the experimental results showing that small rice husk particles increased the mechanical properties of the brake pad (compressive strength, puncture strength, and density). A composite brake pad based on eggshells and gum arabic has also been developed by Edokpia et al. [11]. Eggshell/Gum Arabic-based brake pads showed better characteristics than commercial brake pads [11]. Palm kernel and coconut shell-based brake pads were investigated by Sa'ad et al. [12]. Based on their study, the composite of palm kernel and coconut shell had a suitable characteristic for the brake pad material [12].

Eggshells (Es) are used for the brake pad fabrication since they have the potential to be used as fillers due to their high calcium carbonate ($CaCO_3$) content. Several studies [13,14] have been carried out to investigate the calcium carbonate content of mollusk shells, animal bones, and eggshells. $CaCO_3$ from its natural source, according to these studies, had several properties that make it a suitable reinforcement material for a wide range of applications. Later, it was shown that using $CaCO_3$ materials of varying sizes is an effective method for improving the properties of polymeric materials [13-16]. Then, banana peels (BPs) are also used in brake pad fabrication as they contain natural fibers (such as 60-65% of cellulose, 5-10% of lignin, and 48-59% of lignocellulosic) which are light, have great strength, and stiffness suitable for application as reinforcements [18].

In this study, E and BP were chosen as the reinforcing fillers because of their high $CaCO_3$ and cellulose content. The objective of this study was to investigate how the mechanical properties of brake pads were affected by strengthening eggshell and banana peel particles. The novelty of this study is the combination of two organic waste materials with different mixture ratios for brake pad fabrication. It is expected that this study produces environmentally friendly and affordable brake pads as a substitute for asbestos-based friction materials.

2. Materials and Methods

2.1. Materials

The raw materials for brake pad fabrication include Bisphenol A-epichlorohydrin (resin materials) and cyclo aliphatic amine (hardener), BPs, and Es. BPs and Es here were sourced locally in Bandung, Indonesia.

2.2. Brake Pad Fabrication Step

Before fabricating the brake pads, banana peels and eggshells were prepared to form a powder. Es and BPs were prepared as dual reinforcement of brake pads. Previously, the BPs and Es were cut into small pieces. Then, the BP was dried in an oven at a temperature of 100°C. After that, the BP was dried in an oven at 100°C. The drying process took approximately 2 hours to BP and about 1 hour to the Es. The BPs and Es were ground using a saw-milling apparatus after drying in which the detailed saw-milling apparatus is shown in previous reports [19]. The particles were then placed in a sieve shaker to achieve the desired size following ASTM D1921 (Niaga Kusuma Lestari, Indonesia).

After the BP and E particles have been successfully prepared, the next step was the fabrication of the brake pad using dual reinforcement particles. The brake pad was fabricated by combining E/BP particles with different compositions and mixing them with Bisphenol A-epichlorohydrin. The mixture was stirred for 5 minutes to get a homogeneous mixture. Then, cyclo aliphatic amine was added to the mixture and stirred again for 5 minutes to get a homogeneous paste mixture. The paste mixture subsequently was poured onto a silicon mold (with a dimension is 1×1×1 cm) and the samples were placed in an aerated environment for 14 days to allow them to reach full strength.

In the same way, as a standard, brake pads using single reinforcement of E and BP were also fabricated. In this study, the mass composition of the resin mixture was made at 1:1. Meanwhile, the mass composition of banana peel and eggshell particles was varied. Table 1 summarizes the mass composition of the materials used in the fabrication of brake pads.

Table 1. Mass composition of the raw materials used in the brake pads

Specimen	Composition Percentage (%)				Total (%)
	Bisphenol A-epichlorohydrin	Cyclo-Aliphaticamine	BP	E	
BP	22.22	22.22	55.56	0.00	100
E	22.22	22.22	0.00	55.56	100
E/BP1	22.22	22.22	13.89	41.67	100
E/BP2	22.22	22.22	27.78	27.78	100
E/BP3	22.22	22.22	41.67	13.89	100

2.3. Physical, Chemical, and Mechanical Characterization

A digital microscope was used to investigate the particle size and morphology of the raw material (BP and E particles), the outer surface, and the inner surface of the brake pad samples. Fourier transform infrared was used for chemical characterization to analyze elemental structure products (FTIR, FTIR-6600, Jasco Corp., Japan).

Meanwhile, the mechanical characterization includes:

(i) Compressive and Puncture Strength. The compression test was performed on a Screw Mount Test Instrument (Model I ALX-J, China, ASTM D-2240) equipped with a digital force measuring instrument (Model HP-500, Serial No H5001909262, ASTM D-4713). The brake pad was subjected to a constant rate of 2.6 mm/min during testing. Simultaneously, the compressive force was measured, yielding a curve that depicted the texture profile. The maximum point of the compressive stress-strain curve was then used to calculate compressive strength. Furthermore, during the test, the maximum applied force (in Newtons/square millimeter (N/mm^2) was used to determine the hardness of the sample. A Shore Durometer was used to conduct the puncture strength test (Shore A Hardness, in size, China). During the test, a probe was used to puncture the brake pads. Hardness meanwhile was measured on a scale from 0 to 100.

(ii) Specific Gravity. The specimens' specific gravity was calculated by dividing the unit weight of brake pad material by the unit weight of water. The formula of specific gravity is shown in equation (1).

$$\text{Specific Gravity } (g/cm^3) = mass/volume \quad (1)$$

(iii) Friction Test. The brake pad was polished before friction testing to remove the resin layers on the surface of the

brake pad. The brake pad was tested for friction by sliding it against sandpaper (80 grit; Dae Sung CC-80Cw) with a mass load of 9 kg for 20 minutes at a speed of 25 cm/s. The weight of the brake pads was measured every 2 minutes. Equation (2) was used to calculate the wear rate (M).

$$M = (M_a\text{-}M_b)/(S\times A) \qquad (2)$$

where M_a is the initial weight of the brake pad (g), M_b is the final weight of the brake pad (g), S is the total sliding distance (m), and A is the friction cross-section area (mm^2). The friction coefficient (μ) was the ratio of friction force (f; Newton) to applied force (N; Newton), as expressed in Equation (3).

$$\mu = f/N \qquad (3)$$

3. Results and Discussion

3.1. Bibliometric analysis of brake pad study

The bibliometric study described here examines the developmental analysis of brake pad research. Detailed information using bibliometric analysis is reported in our previous study [20]. This bibliometric analysis seeks to analyze and discover the results of research, the interaction between science and technology, mapping the field of science, tracking/tracing the development of new knowledge in a specific field, and serving as a future indicator in providing more profit competitive in strategic planning [21-25]. Here, a bibliometric analysis of the brake pad study was conducted for 6 periods from 2017 to 2022.

Research on brake pads increased significantly during the first three-year period (2017-2019). From 2017 to 2019, there were respectively 26, 36, and 66 articles about brake pads. However, there was a 17% decrease in the number of articles on brake lining studies in 2020 bringing the total number of articles with related content to 42. Then, in 2021, there was another increase with the number of articles about brake pads remaining the same as in 2019. Furthermore, the number of articles again decreased in 2022 with only 7 articles about brake pads available. Because the data for this study were collected at the beginning of 2022, the number of articles published per year decreased in 2022.

Figure 1 shows network visualization based on co-word mapping on the brake pad topic. VOS viewer was used for co-word mapping analysis based on setting the minimum number of occurrences of keywords as 5 and the threshold was 60. Network visualization (figure 1) shows five clusters correlated with the brake pad study topic. The details of the five clusters are described as follows:

(i) Cluster 1 is marked in red that contains 6 items, including banana peel, banana peel powder, composition, friction, phenolic resin, and polymer composite.
(ii) Cluster 2 is the green one, which contains 5 items including an automobile brake pad, bagasse, palm kernel fiber, production, and reinforcement.
(iv) Cluster 3 is shown in blue, which has 5 items including automobile, brake pad application, characterization, commercial brake pad, and new brake pad.
(v) Cluster 4 is yellow visualization that contains 4 items, namely asbestos-free brake pad, blade, influence, and temperature.
(vi) Cluster 5 is shown in yellow which has 5 items including automobile, brake pad application, characterization, commercial brake pad, and new brake pad.

Based on figure 1, it can be seen that the keywords "production" and "friction" have a larger circle size compared to other keywords, indicating that keywords are the most numerous.

Previous results showed the number of related articles for the last 6 years (2017-2022). Table 2 shows the most relevant research and development research that needs to be cited. The data in Table 2 show publication data on brake pads from the 14 most cited articles (quoted more than 20 times) from 2017 to 2022. Based on table 2, some articles have more than 40 citations and even more than 240 times.

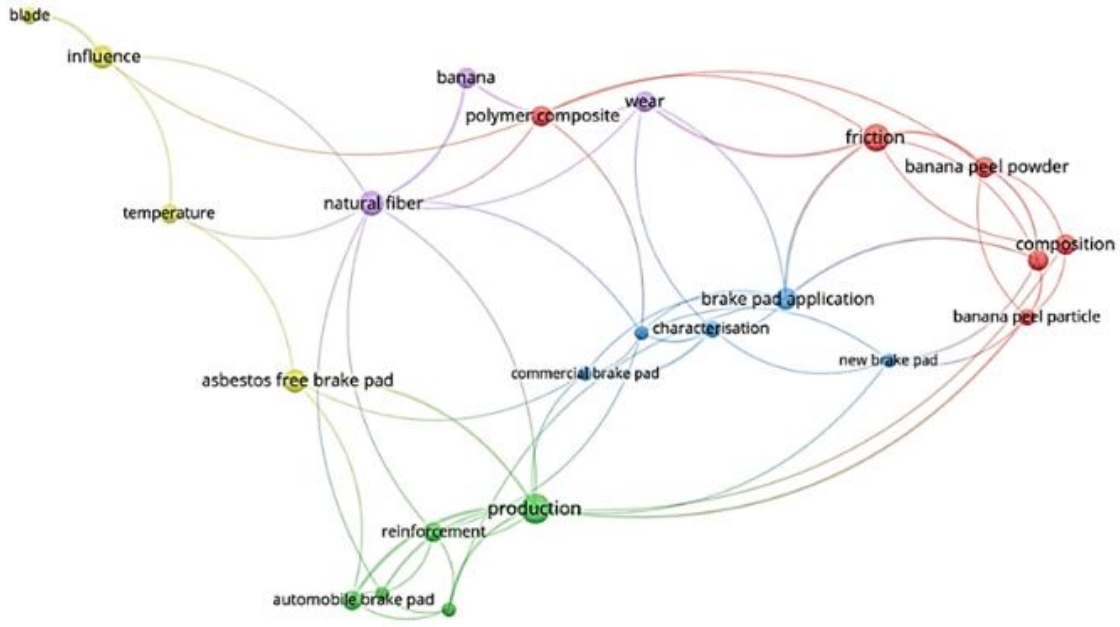

Fig. 1. Network visualization based on co-word

Table 2. Publication data on brake pad study from the 14 articles cited the most in the 2017-2021 period

Author(s) (year)	Title	Reference	Journal
Zhen-Yu et al. (2019)	Influence of banana fiber on physicomechanical and tribological properties of phenolic based friction composites	21	Materials Research Express
Rashid et al. (2017)	Effect of treatments on the physical and morphological properties of SPF/phenolic composites	21	Journal of Natural Fibers
Oladele et al. (2020)	Polymer-based composites: an indispensable material for present and future applications	21	International Journal of Polymer Science
Sumithra and Sidda Reddy (2018)	A review on tribological behaviour of natural reinforced composites	22	Journal of Reinforced Plastics and Composites
Abutu et al. (2019)	Effects of process parameters on the properties of brake pad developed from seashell as reinforcement material using grey relational analysis	29	Engineering science and technology, an international journal
Zwawi (2021)	A review on natural fiber bio-composites, surface modifications and applications	29	Molecules
Liu et al. (2018)	Natural fibre reinforced non-asbestos organic non-metallic friction composites: effect of abaca fibre on mechanical and tribological behaviour	30	Materials Research Express
Akıncıoğlu et al. (2018)	Determination of friction-wear performance and properties of eco-friendly brake pads reinforced with hazelnut shell and boron dusts	32	Arabian Journal for Science and Engineering
Singaravelu et al. (2019)	Development and performance evaluation of eco-friendly crab shell powder based brake pads for automotive applications	32	International Journal of Automotive and Mechanical Engineering
Mahari et al. (2021)	Valorization of municipal wastes using co-pyrolysis for green energy production, energy security, and environmental sustainability: A review	32	Chemical Engineering Journal
Aisyah et al. (2021)	A comprehensive review on advanced sustainable woven natural fibre polymer composites	39	Polymers
Bello et al. (2017)	Study of tensile properties, fractography and morphology of aluminium (1xxx)/coconut shell micro particle composites	45	Journal of King Saud University-Engineering Sciences
Singh et al. (2017)	Assessment of braking performance of lapinus–wollastonite fibre reinforced friction composite materials	53	Journal of King Saud University-Engineering Sciences
Thyavihalli Girijappa et al. (2019)	Natural fibers as sustainable and renewable resource for development of eco-friendly composites: a comprehensive review	244	Frontiers in Materials

3.2. Physicochemical Properties of Brake Pad

Fourier transform infrared spectroscopy (FTIR) is an effective method for describing organic and inorganic compound interaction, as well as analyzing the function group of different elements [26]. Figure 2 shows the FTIR spectrum of all brake pad specimens. There is no discernible difference in spectrum between the five brake pad samples.

The interaction between different elements of the brake pad material was seen in the range of 4000 to 500 cm^{-1}, indicating a band spectrum of banana fiber, eggshell, phenolic resin, and other elements. Based on the results of FTIR analysis, the five brake-pad specimens had absorption bands in the range of 3395-3000 cm^{-1} which is a characteristic of O-H stretching vibrations [26] (see Figures 2(a-e)).

The presence of an absorption band in the wavelength range of 2930-2885 cm^{-1} was related to C-H stretching [27]. For brake pads that were dominated by BP (see Figures 2(a and e)), in this wavelength range, a high amount of lignin and hemicellulose was indicated. The high amount of lignin and hemicellulose in BP and ES/BP3 specimens were indicated with high intensity. For the brake pad it was dominated by ES content (see Figures 2(b, c, and d)). In this wavelength range, it is indicated the presence of insoluble and soluble protein with a lower amount (lower intensity).

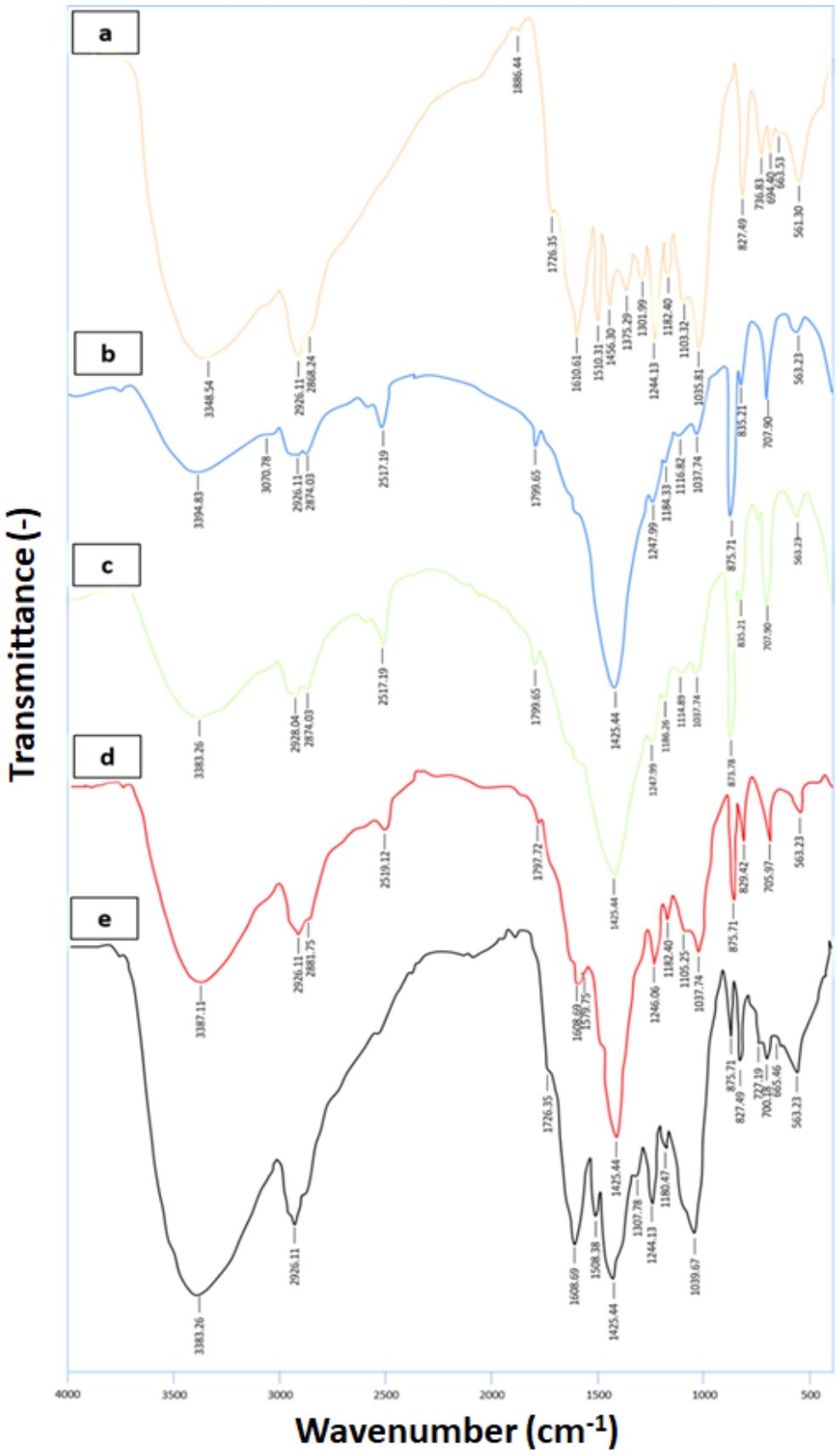

Fig. 2. FTIR spectrum of fabricated brake pad in several samples: (a) BP; (b) ES; (c) ES/BP1; (d) ES/BP2; and (e) E/BP3

The absorption band at 1800-1700 cm^{-1} showed the carbonyl stretching (C=O) vibration. In all four brake pad specimens (BP, ES/BP1, ES/BP2, ES/BP3) except E brake pad specimens, the existence of this C=O group showed the ester group bond in hemicellulose or carboxylic acids in lignin [28]. The absorption band around 1610 cm^{-1} was also related to the stretching of the carbonyl group (amide). Then, the five brake pad specimens also had absorption bands in the 1700-1500 cm^{-}

^{1} area showing stretching of the C=C aromatic ring of phenolic resin [29].

The absorption band in the 1460-1300 cm^{-1} region corresponded to the CH_2 symmetrical bending of the lignin [28]. This absorption band was identified in the BP and E/BP3 brake pad specimens (see figure 2(a and e)). Meanwhile, in E, E/BP1, and E/BP3 specimens, there was a band with high intensity at 1425.44 cm^{-1} indicating the presence of calcium carbonate (see figure 2(b, c, and d)) [29].

The peak in the absorption range of ~1250 cm^{-1} was related to C-O stretching [28]. Then, shifts in the region of ~1040 cm^{-1} (see Figure 3(a, c, d, and e)) showed the β-glycosidic linkage between sugar units in cellulose and hemicelluloses for four brake pad specimens (BP, E/BP1, E/BP2, and E/BP3). Also, there were two peaks observed at ~700 and 876 cm^{-1} in the E, E/BP1, E/BP2, and E/BP3 specimens associated with in-plane deformation and out-plane deformation where each of these absorptions indicated the presence of $CaCO_3$ [29] (see figure 2(b, c, d, and e)). The existence of $CaCO_3$ can possibly give additional excellent performance to the product [30].

As seen in Figure 2, the brake pad specimen labeled E/BP1 (see figure 2(c)) and E/BP2 (see figure 2(d)) had almost the same spectrum as the E brake pad specimen (see figure 2(b)) because specimens E/BP1 and E/BP2 had a higher ratio of filler mixture to E particle content. In contrast, the E/BP3 specimen (see figure 2(e)) had a similar spectrum to the BP specimen (see figure 2(a)) due to the higher ratio of filler mixture to BP particle content. The comparison of each functional group for each specimen is summarized in Table 3.

Figures 3(a and c) illustrates the microscopy images of BP and E particles, respectively. The BP and E particles showed inhomogeneous particle sizes (see figures 3(a and c)). The particle sizes of BP and E particles were analyzed using Feret analysis as shown in figures 3(b and d). The results of Feret's analysis showed that the BP particle size was in the range of 100-500 μm with an average size of 245 μm (see figure 3(b)). For E particles, the particle size ranged from 34 to 500 μm with an average size of 262 μm (see figure 3(d)). To confirm the microstructure, further analysis using electron microscope must be done [31] in which this will be done in our future studies.

Figures 4 (a-e) show the fabricated brake pad based on BP, E, E/BP1, E/BP2, and E/BP3, respectively. Brake pads that have been fabricated had a striking color difference. The BP and E/BP3-based brake pads had almost the same color i.e. black. For the others, the E-based brake pad was in cream color, the E/BP1-based brake pad had a brown color, and the E/BP2-based brake pad had a dark brown color. From the microscope image, there were yellow and black areas that indicated BP particles, the white areas were E particles, and the shiny areas were resin

Table 3. The wavelength of peak used for FTIR analysis and its corresponding functional groups

Wavenumber (cm^{-1})	Samples				
	BP	E	E/BP1	E/BP2	E/BP3
3395-3000	O-H stretching	O-H stretching	O-H stretching	O-H stretching	O-H stretching
2930-2885	C-H stretching indicated the high amount of lignin and hemicellulose	C-H stretching indicated the high amount of lignin and hemicellulose	C-H stretching indicated the high amount of lignin and hemicellulose	C-H stretching indicated the high amount of lignin and hemicellulose	C-H stretching indicated the high amount of lignin and hemicellulose
1800-1700	C=O stretching shows the ester group bond in hemicellulose / carboxylic acids in lignin	-	C=O stretching shows the ester group bond in hemicellulose / carboxylic acids in lignin	C=O stretching shows the ester group bond in hemicellulose / carboxylic acids in lignin	C=O stretching shows the ester group bond in hemicellulose / carboxylic acids in lignin
1610	C=O stretching for amide	-	C=O stretching for amide	C=O stretching for amide	C=O stretching for amide
1700-1500	C=C aromatic ring of phenolic resin	C=C aromatic ring of phenolic resin	C=C aromatic ring of phenolic resin	C=C aromatic ring of phenolic resin	C=C aromatic ring of phenolic resin
1460-1300	CH_2 symmetrical bending of the lignin	-	-	-	CH_2 symmetrical bending of the lignin
1425.44	-	the presence of calcium carbonate	the presence of calcium carbonate	the presence of calcium carbonate	-
~1250	C-O stretching	C-O stretching	C-O stretching	C-O stretching	C-O stretching
~1040	β-glycosidic linkage between sugar units in cellulose and hemicelluloses	-	β-glycosidic linkage between sugar units in cellulose and hemicelluloses	β-glycosidic linkage between sugar units in cellulose and hemicelluloses	β-glycosidic linkage between sugar units in cellulose and hemicelluloses
~700-876	-	Presence in-plane deformation and out-plane deformation where each of these absorptions indicates the presence of $CaCO_3$	Presence in-plane deformation and out-plane deformation where each of these absorptions indicates the presence of $CaCO_3$	Presence in-plane deformation and out-plane deformation where each of these absorptions indicates the presence of $CaCO_3$	Presence in-plane deformation and out-plane deformation where each of these absorptions indicates the presence of $CaCO_3$

The surface appearance (outer and inner) of the brake pads show that all the fabricated brake pads have an uneven surface and have pores (see figures 4(f-o)). Based on observations, brake pads based on E or brake pads that have a high content of E particles had smoother inner and outer surfaces than other specimens. Therefore, the use of E particles for the brake pad resulted in smoother structures in the final product. Of all the brake pads successfully fabricated, E particles were visible filling the resin-based brake pads homogeneously.

Figure 5 shows the specific gravity characteristics of the brake pad to support the analysis of the texture profile on the brake pad. Based on the specific gravity plot, the brake pad specimen with the highest E particle content had the highest specific gravity value, i.e. 0.048 and 0.047 for E and E/BP1 specimens, respectively. A high specific gravity value was correlated with a more homogeneous reinforcement particle packing level in the brake pad composite matrix phase [31], thus, it is associated with the most acceptable acceptance impact of brake pad characteristics. On the other hand, the specific gravity of other specimens might be better because they are lighter in weight, thus meeting the standards as well. In this case, all specimens have lower specific gravity than commercial brake pads (1.890 g/cm^3) but still meet the standard [31]. Furthermore, another fact demonstrates that, when comparing the two different reinforcements, BP particles are far more suitable as a reinforcement than E particles or even other asbestos, because the overall weight of the sample is reduced.

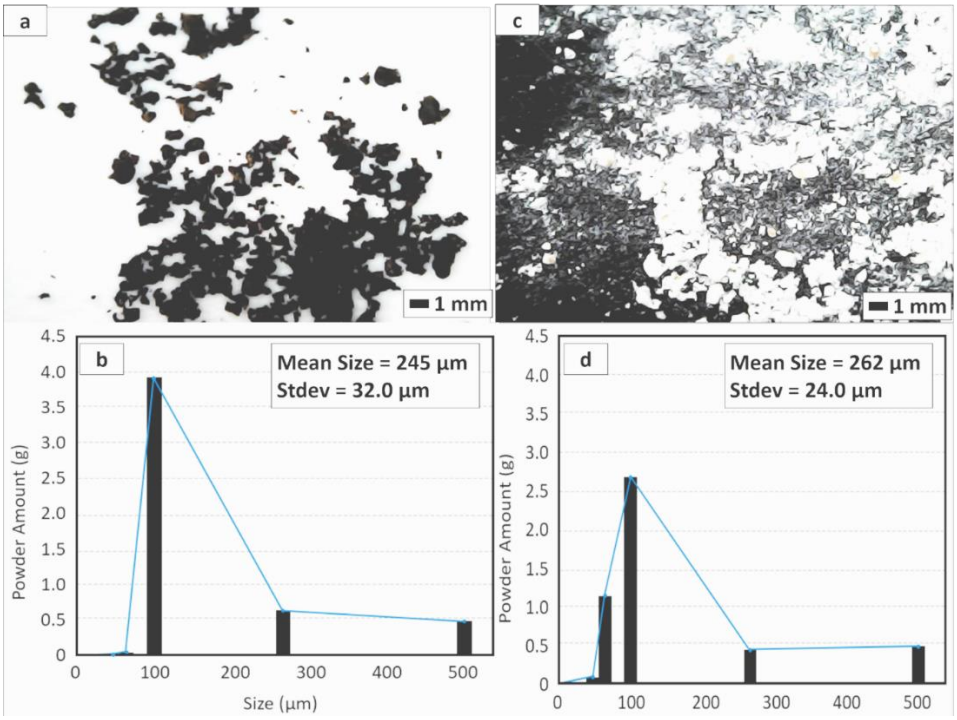

Fig. 3. Photograph images of the particles: (a) BP particles and (b) E particles. Particle size distribution: (c) BP particles and (d) E particles

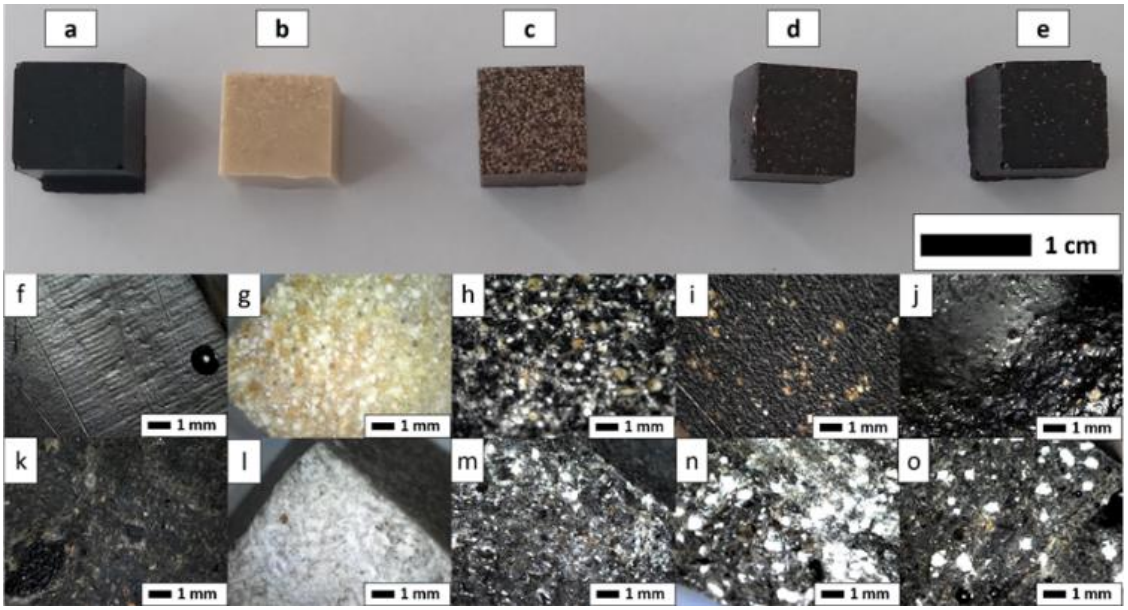

Fig. 4. Photograph image of the successfully fabricated brake pad. Figures (a-e) are the brake pads prepared with BP, E, E/BP1, E/BP2; and E/BP3, respectively. Figures (f-j) are the outer surface of the brake pads; and Figures (k-o) are the inner surface of the brake pads. Figures (f,k), (g,l), (h,m), (i,n), and (j,o) are samples using BP, E, E/BP1, E/BP2, and E/BP3, respectively.

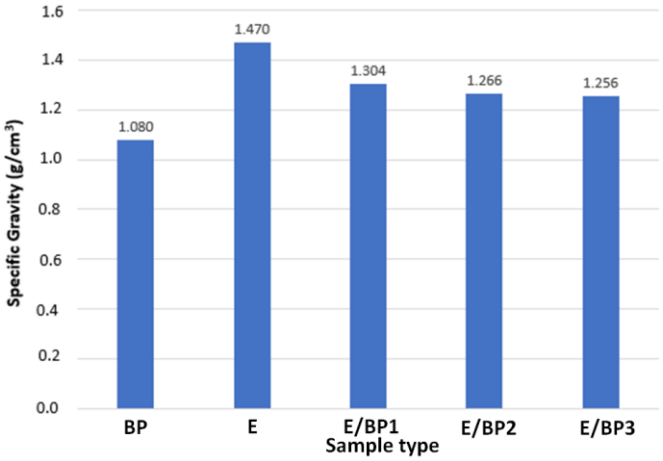

Fig. 5. The plot of specific gravity of the various brake pad specimens prepared by various types of raw materials

3.3. Mechanical Characterization

Figures 6(a and b) show the compressive test results in which the greater compressive resistance in the material is indicated by higher compressive stress obtained from the compressive test. Figure 6(a) shows the highest peak for the E/BP3 specimen and the detailed values for BP, E, E/BP1, E/BP2, and E/BP3 are 1.8; 1.7; 3.9; 4.3; and 4.5, respectively (see figure 6(b)). Thus, based on the compressive test, the hardness of the brake pad specimen was E/BP3.

To confirm the compressive test result, the puncture test was done. The data from the puncture test results are presented in table 4. The puncture test showed that the greater value was obtained when the level of hardness was getting smaller. The specimen hardness value showed the depth of the needle inserted into the specimen. The deeper stab showed a more brittle specimen [33]. The results of this puncture test followed the results of the compression test (figures 6(a and b)) that the brake pad specimen with the best hardness was obtained by the E/BP3 specimen (see table 4). Based on the data from the compressive and puncture test, the brake pad with the composition of BP or E particles only (single reinforcement) had a lower level of hardness when compared to the brake pad, which was fabricated from a mixture of BP and E particles (dual reinforcement). Dual-sized reinforcement was found better than single reinforcement due to the synergistic effect between each pair of reinforcement on the dual reinforcement brake pad [34]. The results are in a good agreement with our previous studies regarding the effect of particle sizes and material types on the mechanical properties (see table 5) [35].

Table 4. Brake pad specimen puncture strength test results

Sample	Durometer Shore A Hardness Scale of Brake Pad
BP	93.80
E	94.60
E/BP1	91.40
E/BP2	88.20
E/BP3	86.80

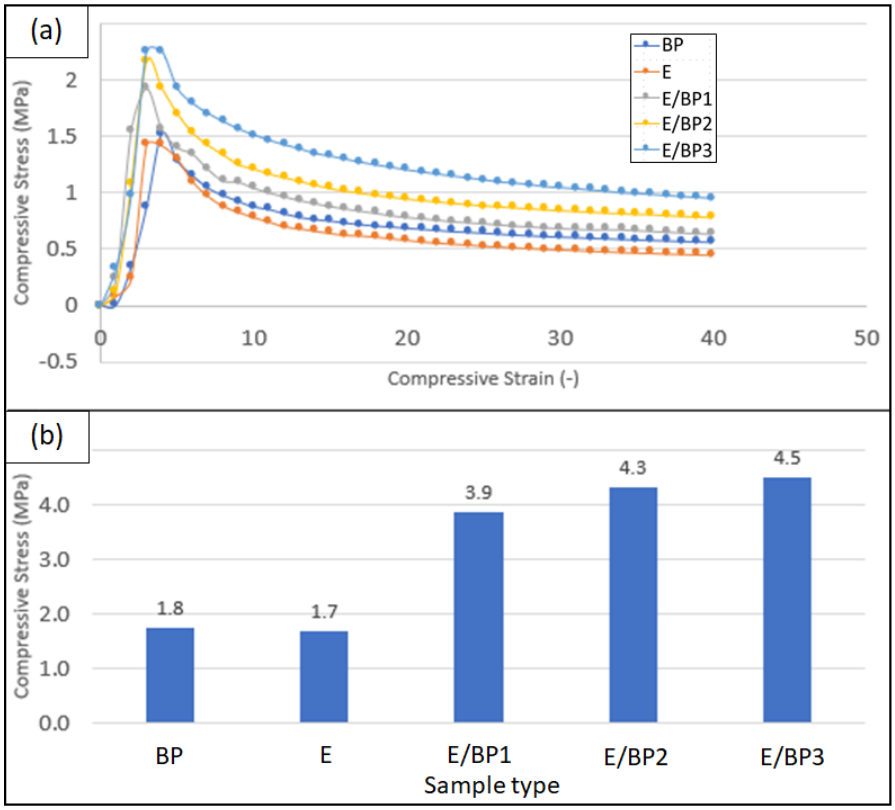

Fig. 6. The compressive test results: (a) compressive stress-strain curves; and (b) compressive strength results

Table 5. The ilustration of dual components in the mechanical properties. Table was adopted from reference [35]

Type	Model	Crack Model
2 particles with different sizes Particle A + Particle B	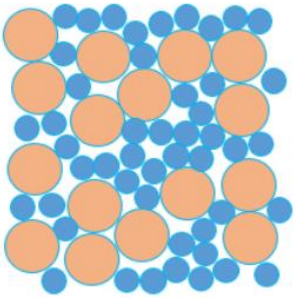	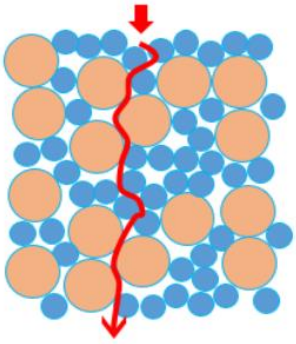
2 particles with almost the same sizes Particle A + Particle B	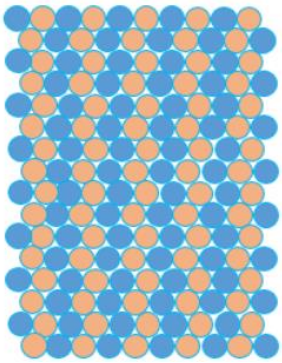	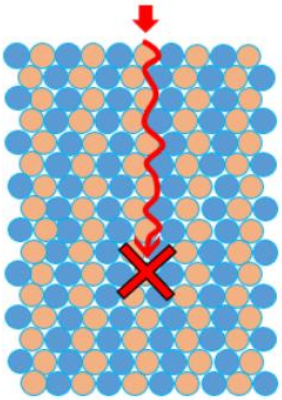

In addition, specifically, brake pads with a high BP particle content and a low E particle content had the best hardness level among others. In this study, it was determined that a higher percentage of E particles in the reinforcement mixture resulted in low hardness. Brittleness was caused by a high percentage of E particles. Meanwhile, a high BP particle ratio in the filler mixture indicated several better brake pad characteristics. It has been mentioned previously that ES mainly contains calcium carbonate ($CaCO_3$) and BP contains natural fibers (cellulose, lignin, and lignocellulose) [28]. Naturally, CaCO3 has brittle characteristics. Therefore, $CaCO_3$ imparts brittleness to the brake pads [36]. Also, the shorter size of $CaCO_3$ compared to carbon fiber (natural fiber) has made the strength of $CaCO_3$ lower than carbon fiber [37]. Meanwhile, natural fiber showed a natural characteristic of mechanical properties such as strength [38]. Therefore, a high ratio of BP particles in the dual reinforcement led to an increase in the bonding ability of the resin, thereby creating good adhesion between the filler and the matrix.

Figure 7 depicts the change in mass of the prepared brake pads during a friction test. During the test, the brake pads were forced to make a contact with sandpaper (as in a brake drum/disc model), converting kinetic energy into heat energy and generating heat and friction [39]. Debris was also produced during this process. The increased mass loss was due to a decrease in the hardness characteristics caused by a decrease in the BP particle ratio in the dual reinforcement.

Table 6 shows the mass loss rate, wear rate, and friction coefficient of the brake pad in detail. A lower mass-loss rate corresponded to a lower wear rate and higher friction coefficient. Brake pads with high BP particles and low E particles composition (E/BP3) had a lower mass rate and higher friction coefficient (see Table 6). In short, the friction coefficients of the brake pads made of BP, E, E/BP1, E/BP2, and E/BP3 were 1.53×10^{-4}, 1.50×10^{-4}, 1.52×10^{-4}, 1.60×10^{-4}, and 1.67×10^{-4}, respectively. Meanwhile, the coefficient of friction of the commercial brake lining was 1.4×10^{-4}. Here, we compared the friction test results of all fabricated brake pads with those of commercial brake pads. The E/BP3 specimen was found as the best specimen of all fabricated brake pads and commercial brake pads. Based on the test results of mass loss, friction rate, and coefficient of friction, here, all samples showed better characteristics than commercial brake pads.

Based on this study, brake pads with a lower mass-loss rate and higher friction coefficient characteristics were those with the hardness characteristic. These results are in agreement with the literature [40] that a higher hardness material typically has a lower mass loss and higher friction coefficient than a lower hardness material. In terms of hardness, mass loss, and friction coefficient of the brake pad specimens, all dual reinforcement of brake pad specimens exhibited better characteristics compared to single reinforcement of brake pads. That meant there was a synergistic effect between each pair of reinforcement on the dual reinforcement brake pads [34].

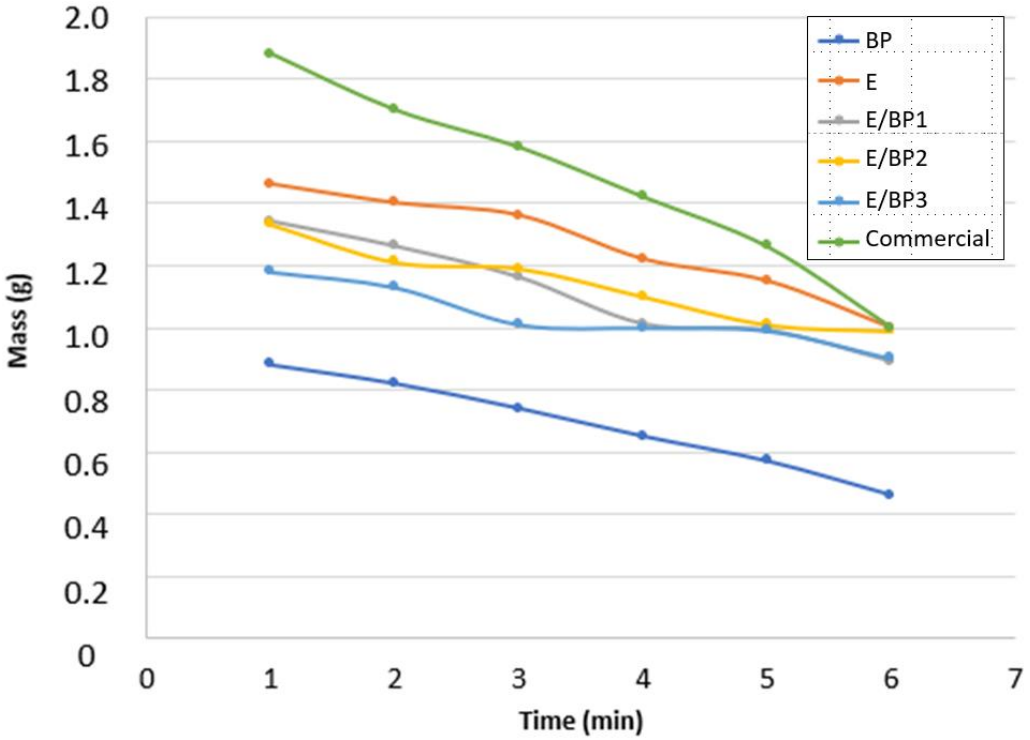

Fig. 7. The change of mass of fabricated brake pad during friction test

Table 6. Mass loss rate, wear rate, and friction coefficient of specimens with different compositions

Sample	Initial Mass (g)	Final Mass (g)	Mass loss rate (%)	Standard Deviation of mass loss (g)	t (s)	A (mm^2)	Wear Rate ($g/s.mm^2$) ($\times 10^{-4}$)	Friction Coefficient ($\times 10^{-4}$)
BP	0.88	0.46	42	0.126	300	100	0.140	1.53
E	1.46	1.00	46	0.144	300	100	0.154	1.50
E/BP1	1.34	0.89	46	0.131	300	100	0.150	1.52
E/BP2	1.33	0.99	34	0.089	300	100	0.110	1.60
E/BP3	1.18	0.90	28	0.073	300	100	0.093	1.67
Commercial	1.88	1.00	88	0.246	300	100	0.290	1.40

3.4. *Techno-Economic Analysis for The Production Analysis*

Techno-economic analysis of brake pad production was performed to assess the project's engineering and economic feasibility. From an engineering perspective, raw materials were calculated based on mass balance during the manufacturing process. The economic evaluation used several assumptions based upon equipment specifications, raw material/chemical prices, utility systems, and equipment costs obtained from various e-commerce sites such as Alibaba, Amazon, Tokopedia, and others. The data were then processed, used, inputted, and computerized in the economic feasibility analysis calculation. Here, the techno-economic analysis was performed under ideal conditions. The detailed economic feasibility analysis calculations were explained in our previous studies [41-44] in which the calculations were done for estimating gross profit margin (GPM), payback period (PBP), break event point (BEP), internal rate return (IRR), creating net present value (CNPV), return on investment (ROI) and profitability index (PI).

In the calculation, several assumptions included:

(i) The prices of the equipment and raw materials used were obtained from commercially available online markets such as alibaba.com, tokopedia.com, and bukalapak.com.

(ii) For brake pads from E and BP particles (non-asbestos-based brake pads), the raw materials needed included Es, BPs, bisphenol A-epichlorohydrin, and Aliphatic cyclic amine with the composition of 140, 47, 100, and 100 kg/cycle, respectively.

(iii) For brake pads based on asbestos material (asbestos-based brake pad), the raw materials needed included asbestos, barium sulfate ($BaSO_4$), bisphenol A-epichlorohydrin, and Aliphatic cyclic amine with the composition are 140, 47, 100, and 100 kg/cycle, respectively.

(iv) No byproduct during the production process was available. The room temperature was used during the

production process. The final product consisted solely of resin-based brake pad material.

(v) The production of resin-based brake pads required one cycle per day.

(vi) In the mass balance analysis, one producing cycle for one day produced 18,750 pieces of brake pads with dimensions of 4 x 1 x 3 cm in length, height, and weight. Under ideal conditions, the project could be scaled up to 264 cycles per year. As a result, the project's production capacity was 4,950,000 units.

(vii) The unit price was in USD. The USD to Rupiah conversion rate is 1 USD = 15,000.

(viii) Non-asbestos and asbestos-based brake pad costs were two USD per piece.

(ix) Stoichiometry calculations were used to calculate all raw materials used during production.

(x) There was no charge for the egg shell and banana peel.

(xi) The discount rate was 15% and income taxes was 10%.

(xii) The cost for the utility system was 0.10 USD/kWh.

(xiii) The number of productive days of labor in a year is 264.

(xiv) The labor force is composed of 15 persons, each of whom earns 8 USD/day.

(xv) The project took in the newly acquired underground. As a result, the land was calculated as the initial cost of project development, which would be recovered once the project was operational.

(xvi) The project is running for 20 years.

Figure 8 depicts the CNPV/TIC versus lifetime curve for the resin-based brake pad project. Based on the ideal curve, the CNPV/TIC parameter remains negative for the first three years of the project. The project's first two years are still under construction. Variable costs, fixed costs, sales, depreciation, pre-tax profits, and income taxes are all factors influencing this result, which starts to be considered in the third year. The production process has only just begun in the third year, and there is no profit. The project begins to profit in the fourth year and can be profitable for up to 20 years. According to the economic analysis, the resin-based brake pad project is profitable and promising under ideal conditions. Detailed information for the present calculation is reported in our previous studies [1].

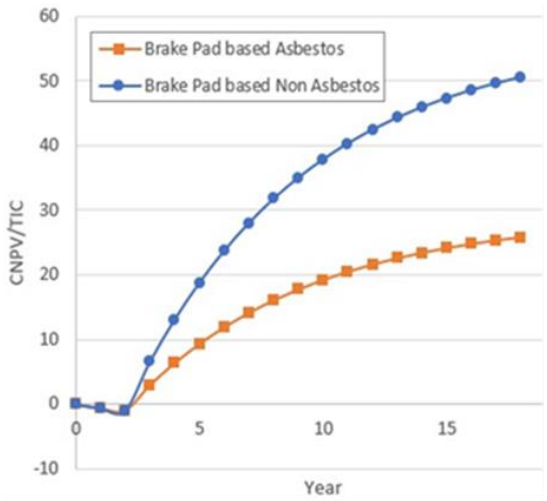

Fig 8.The CNPV/TIC curve against the lifetime for resin-based brake pad project. Figure was adopted from reference [1]

4. Conclusion

The dual reinforcement ratio used to fabricate brake pads affected the mechanical and frictional properties of brake pads. Brake pads fabricated from dual reinforcement had several better mechanical and frictional properties than single filers. In addition to its superior hardness and friction properties compared to single reinforcement, overall the specimens with dual reinforcement had densities between BP and E single-particle reinforcement, indicating that brake pads with dual reinforcement was lighter than single E particle-based brake pads and was heavier than single BP particle-based brake pads. Here, all samples had some better characteristics than commercial brake pads. Then, brake pads with a dual reinforcement labeled as ES/BP3 showed the best hardness and friction properties of the brake pads. The hardness value of the best fabricated brake pad sample was proven by carrying out tests according to ASTM D-2240 and ASTM D-4713 standards. The results of the frictional properties of the fabricated brake pads was done by comparing them with commercial brake pads showing that all samples of the fabricated brake pads had better frictional properties than commercial brake pads. Overall, the increase in the particle composition of BP as a reinforcement, which was modified by the addition of a small amount of E particles could increase the strength and frictional properties of brake pads. A high BP particle ratio here had a dominant role in dual reinforcement, which could increase the bonding ability of the resin, thus producing good adhesion between the filler and the matrix. The techno-economic analysis also confirmed the prospective production of brake pads from E and BP particles (compared to commercial brake pads).

Acknowledgments

This study acknowledged Bangdos Universitas Pendidikan Indonesia and RISTEK DIKTI for Grant-in-aid Penelitian Terapan Unggulan Perguruan Tinggi (PTUPT).

References

1. M. A. Maleque, A. Atiqah, R. J. Talib and H. Zahurin, *New natural fibre reinforced aluminium composite for automotive brake pad*, Int. J. Mech. Mater. Eng., 7(2) (2012) 166-170.
2. D. S. E. A. Chan and G. W. Stachowiak, *Review of automotive brake friction materials*, P I MECH ENG D-J AUT, 218(9) (2004) 953-966.
3. D. Kolluri, A. K. Ghosh and J. Bijwe, *Analysis of load-speed sensitivity of friction composites based on various synthetic graphites*, Wear, 266(1-2) (2009) 266-274.
4. G. Ak?nc?o?lu, H. Öktem, I. Uygur and S. Ak?nc?o?lu, *Determination of friction-wear performance and properties of eco-friendly brake pads reinforced with hazelnut shell and boron dusts*, Arab. J. Sci. Eng., 43(9) (2018) 4727-4737.
5. W. B. Wannik, A. F. Ayob, S. Syahrullail, H. H. Masjuki and M. F. Ahmad, *The effect of boron friction modifier on the performance of brake pads*, Int. J. Mech. Mater. Eng., 7(1) (2012) 31-35.
6. A. B. D. Nandiyanto, S. N. Hofifah, G. C. S. Girsang, S. R. Putri, B. A. Budiman, F. Triawan, et al, *The effects of rice husk particles size as a reinforcement component on resin-based brake pad performance: From*

literature review on the use of agricultural waste as a reinforcement material, chemical polymerization reaction of epoxy resin, to experiments, AE., 4(2) (2021) 68-82.

7. R. O. Edokpia, V. S. Aigbodion, C. U. Atuanya, J. O. Agunsoye and K. Mu'azu, *Experimental study of the properties of brake pad using eggshell particles–Gum Arabic composites*, J Chinese Adv Mater Soc.ens, 4(2) (2016) 172-184.
8. H. Sa'ad, B. D. Omoleyomi, E. A. Alhassan, E. O. Ariyo and T. Abadunmi, *Mechanical performance of abrasive sandpaper made with palm kernel shells and coconut shells*, J. Mech. Behav. Mater., 30(1) (2021) 28-37.
9. T. P. Mohan, K. Kanny, *Thermal, mechanical and physical properties of nanoeggshell particle-filled epoxy nanocomposites*, J. Compos. Mater., 52(29) (2018) 3989-4000.
10. J. R. Woodard, A. J. Hilldore, S. K. Lan, C. J. Park, A. W. Morgan, J. A. C. Eurell, et al, *The mechanical properties and osteoconductivity of hydroxyapatite bone scaffolds with multi-scale porosity*, Biomaterials, 28(1) (2007) 45-54.
11. T. A. Hassan, V. K. Rangari and S. Jeelani, *Mechanical and thermal properties of bio?based CaCO3/soybean?based hybrid unsaturated polyester nanocomposites*, J. Appl. Polym. Sci., 130(3) (2013) 1442-1452.
12. O. J. Gbadeyan, S. Adali, G. Bright, B. Sithole, B., and O. Awogbemi, *Studies on the mechanical and absorption properties of achatina fulica snail and eggshells reinforced composite materials*, Compos. Struct., 239 (2020) 112043.
13. U. D. Idris, V. S. Aigbodion, I. J. Abubakar and C. I. Nwoye, *Eco-friendly asbestos free brake-pad: Using banana peels*, J. King Saud Univ. Eng. Sci., 27(2) (2015) 185-192.
14. S. Yashwhanth, M. M. Mohan, R. Anandhan and S. K. Selvaraj, *Present knowledge and perspective on the role of natural fibers in the brake pad material*, Materials Today: Proceedings, 46 (2021) 7329-7337.
15. A. B. D. Nandiyanto, R. Andika, M. Aziz and L. S. Riza, *Working volume and milling time on the product size/morphology, product yield, and electricity consumption in the ball-milling process of organic material*, Indones. J. Sci. Technol., 3(2) (2018) 82-94.
16. A. B. D. Nandiyanto, R. Zaen and R.Oktiani, *Working volume in high-energy ball-milling process on breakage characteristics and adsorption performance of rice straw ash*, Arab. J. Sci. Eng., 43(11) (2018) 6057-6066.
17. Y. Sukrawan, A. Hamdani and S.A. Mardani, *Effect of bamboo weight faction on mechanical properties in non-asbestos composite of motorcycle brake pad*, Mater. Phys. Mech., 42(3) (2019) 367-372.
18. A. B. D. Nandiyanto, M. K. Biddinika and F. Triawan, *Evaluation on research effectiveness in a subject area among top class universities: a case of Indonesia's academic publication dataset on chemical and material sciences*, J. Eng. Sci. Technol, 15(3) (2020) 1747-1775.
19. H. Soegoto, E. S. Soegoto, S. Luckyardi and A. A. Rafdhi, (2022). *A Bibliometric Analysis of Management Bioenergy Research Using Vosviewer Application*, Indones. J. Sci. Technol., 7(1) (2022) 89-104.
20. A. B. D. Nandiyanto and D. F. Al Husaeni, *A bibliometric analysis of materials research in Indonesian journal using VOSviewer*, J. Eng. Res., (2021).
21. R. Ragadhita and A. B. D. Nandiyanto, *Computational Bibliometric Analysis on Publication of Techno-Economic Education*, Indo. J. Multidicip. Res., 2(1) (2022) 213-220.
22. A. B. D. Nandiyanto, D. N. Al Husaeni, D. F. Al Husaeni, *A bibliometric analysis of chemical engineering research using vosviewer and its correlation with covid-19 pandemic condition*, J. Eng. Sci. Technol, 16(6) (2021) 4414-4422.
23. A. B. D. Nandiyanto, R. Oktiani and R.Ragadhita, *How to read and interpret FTIR spectroscope of organic material*, Indones. J. Sci. Technol., 4(1) (2019) 97-118.
24. S. Kamsonlian, S. Suresh, C. B. Majumder and S. Chand, *Characterization of banana and orange peels: biosorption mechanism*, Int. j. sci. technol. manag., 2(4) (2011) 1-7.
25. L. Mohammed, M. N. Ansari, G. Pua, M. Jawaid and M. S. Islam, *A review on natural fiber reinforced polymer composite and its applications*, Int. J. Polym. Sci., (2015).
26. N. A. A. N. Yusuf, M. K. A. A. Razab, N. Hakimin, M. Kamal, N. Ameram, M. N. A. Nordin, *Characterization of Bio-Polymer Composite Thin Film Based on Banana Peel and Eggshell*, Int. j. curr. eng. technol., Malaysia (2018).
27. I. M. De Rosa, J. M. Kenny, M. Maniruzzaman, M. Moniruzzaman, M. Monti, D. Puglia et al, (2011). *Effect of chemical treatments on the mechanical and thermal behaviour of okra (Abelmoschus esculentus) fibres*, Compos. Sci. Technol., 71(2) (2011) 246-254.
28. M. S. Tizo, L. A. V. Blanco, A. C. Q. Cagas, B. R. B. D. Cruz, J. C. Encoy, J. V. Gunting and V. I. F. Mabayo, *Efficiency of calcium carbonate from eggshells as an adsorbent for cadmium removal in aqueous solution*, Sustain. Environ. Res., 28(6) (2018) 326-332.
29. R. O. Edokpia, V. S. Aigbodion, O. B. Obiorah and C. U. Atuanya, *WITHDRAWN: Evaluation of the properties of ecofriendly brake pad using eggshell particles–Gum Arabic*, (2014)
30. N. A. Ademoh and A. I. Olabisi, (2015). *Development and evaluation of maize husks (asbestos-free) based brake pad*, Development, 5(2) (2015) 67-80.
31. S. Anggraeni, R. Maulida, R. Ragadhita, S. N. Hofifah and A. B. D. Nandiyanto, *Teaching the Effect of Liming Concentration on Mechanical Characteristics of Cowhide Crackers for Senior High School Students*, J. Eng. Educ. Transform., 34(Special Issue) (2021).
32. P. K. Chattopadhyay, U. Basuli and S. Chattopadhyay, *Studies on novel dual filler based epoxidized natural rubber nanocomposite*, Polym. Compos., 31(5) (2010) 835-846.
33. N. A. A. N. Yusuf, M. K. A. A. Razab, M. B. A. Bakar, K. J. Yen, C. W. Tung, R. S. M. Ghani, et al, *Determination of structural, physical, and thermal properties of biocomposite thin film from waste banana peel*, J. Teknol., 81(1) (2019).
34. L. I. Ming, L. Meng, Y. A. N. G. Yuanyi, Y. L. Zaoyuan and G. Xiaoyang, *Mechanical properties of oil well cement stone reinforced with hybrid fiber of calcium carbonate whisker and carbon fiber*, Pet. Explor. Dev., 42(1) (2015) 104-111.
35. Zwawi, M, *A review on natural fiber bio-composites, surface modifications and applications. Molecules*, 26(2) (2021) 404.
36. R. Hinrichs, M. R. Soares, R. G. Lamb, M. R. Soares and M. A. Z. Vasconcellos, *Phase characterization of debris generated in brake pad coefficient of friction tests*, Wear, 270(7-8) (2011) 515-519.
37. S. Sheng, H. Zhou, X. Wang, Y. Qiao, H. Yuan, J. Chen and J. Li, *Friction and Wear Behaviors of Fe-19Cr-15Mn-0.66 N Steel at High Temperature*, Coatings, 11(11) (2021) 1285.